# SPECTRAL EFFECTS ON STRESS RELAXATION OF INCONEL X-750 SPRINGS IN CANDU® REACTORS

by

*M. Griffiths, F.J. Butcher, I. Ariani and S. Douglas*
*Atomic Energy of Canada Ltd., Chalk River, Ontario, Canada*
*and*
*F.A. Garner and L. Greenwood*
*Batelle, Pacific North West Laboratory, Richland, Washington*

## ABSTRACT

CANDU® reactors have been operating for periods up to about 25 years. During this time there are changes to the nuclear reactor core components that are a function of operating environment and time. It is important to know how the properties of critical core components are likely to change over the life of a reactor and therefore their behaviours are characterised long before the end of the reactor design life.

Tests are typically conducted in materials test reactors. The behaviour of a material is often characterised as a function of fast neutron fluence and the expected effect of operating time is established by simply extrapolating as a function of fluence. This may be appropriate when the neutron energy spectrum for the materials test reactor matches closely the neutron spectrum where the component resides in the power reactor. However, in cases where the spectrum is very different one has to convert the accumulated dose into a unit that is common in its effect on the material properties. For many property changes in nuclear reactor cores this unit is displacements per atom (dpa). There are different processes that cause atomic displacements and the main ones have to be included in any dpa calculation in order to accurately predict how a given component will perform.

One property that is significantly affected by irradiation is stress. Irradiation-induced stress relaxation is a phenomenon that has been used as a method for studying in-reactor creep. Stress relaxation also results in a loss of tension in springs if these springs are in a reactor core environment. This paper describes the stress relaxation of Inconel X-750 in the National Research Universal (NRU) materials test reactor and relates this to the expected relaxation of springs that are installed in the periphery of CANDU reactors. The results show that spectral effects are particularly significant for certain components at the edge of the CANDU reactor core where the neutron spectrum is changing significantly. The effect of transmutation can also be important in modifying the damage rate. The production of Ni-59 in alloys containing Ni has a significant effect on the amount of radiation damage produced when the thermal neutron flux is high. The effect of gamma radiation is also considered and shown to be small even when the gamma flux is high relative to the neutron flux.

---

® CANDU is a registered trademark of Atomic Energy of Canada Limited (AECL).

# 1. Introduction

## 1.1 Materials

In a CANDU[1] reactor, the fuel bundles and primary coolant are contained within Zr-2.5Nb pressure tubes that are approximately 6.3 metres in length, have an internal diameter of 104 mm and a wall thickness of 4.2 mm. The number of fuel channels varies depending on the type of reactor; the CANDU 6 design has 380 fuel channels producing a total electrical power output of about 700 MW. During service the pressure tubes operate at temperatures between about 538K and 583K, and with inlet coolant pressures up to 11.5 MPa corresponding to initial hoop stresses of 140 MPa. The maximum flux of fast neutrons from the fuel is about $4 \times 10^{17}\ n \cdot m^{-2} \cdot s^{-1}$, E > 1 MeV. Components within the reactor core experience displacement damage rates such that each atom is displaced about once every year. The damage rates at the edge of the core are substantially less but are nevertheless important when small amounts of damage can affect certain physical properties of the reactor components.

Inconel X-750 springs are used to provide tension to vertical reactivity mechanism guide tubes in some CANDU reactors. The springs reside at the edge of the reactor core and operate at a temperature of about 350K. At this temperature it is assumed that thermal creep is negligible [1]. They are exposed to a very low dose of fast neutrons over the lifetime of the reactor. However, because the thermal neutron flux is relatively high at the edge of the core the radiation damage resulting from the thermal neutron and also the gamma flux has to be assessed in order to determine the relaxation rate expected in these components based on measurements from tests in a materials test reactor.

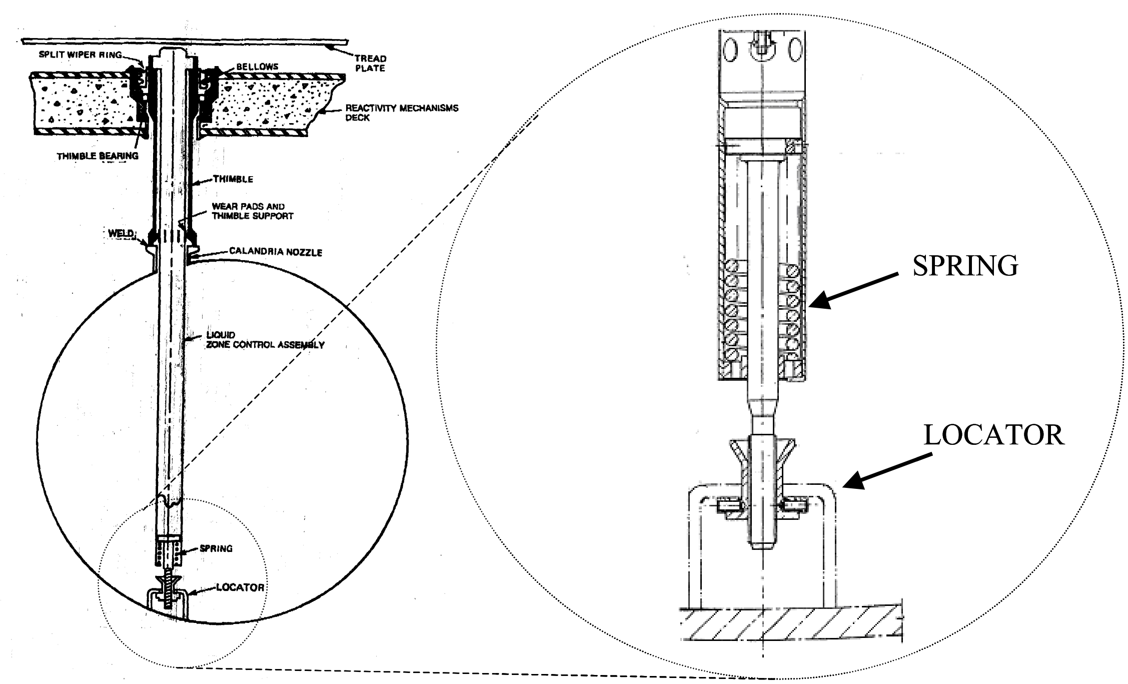


1 Schematic diagram showing location and configuration of the Inconel X-750 guide tube tensioning spring.

[1] CANDU is a registered trade-mark of Atomic Energy of Canada Limited (AECL).

Materials under stress, and subject to neutron irradiation, experience irradiation-enhanced stress relaxation. Bent-beam stress-relaxation tests provide a means of assessing the relaxation behaviour. By assuming that stress relaxation is equivalent to creep under decreasing stress the irradiation-enhanced creep rate can be derived from tests in which small elastically constrained beams are exposed to neutron irradiation.

The rate at which elastic strain, *e*, is converted to plastic strain is given by, $\dot{\varepsilon}$:

$$\dot{\varepsilon} = C\sigma\phi \qquad (1)$$

where $\phi$ is the irradiation flux, and $\sigma = Ee$ is the stress in a specimen with modulus E, deformed to an elastic strain, *e.* C is a temperature- and material-dependent constant, the creep compliance. In this approximation the effect of thermal creep is assumed to be small and is neglected.

For irradiation creep the time dependent remaining elastic stress stress, $\sigma_t$, is related to the creep compliance, C, by:

$$\sigma_t = \sigma_0 \exp(-CE\phi t) \qquad (2)$$

Where $\sigma_o$ is the initial elastic stress [1, 2]. From (2), the creep compliance is derived by plotting $\ln(\sigma_t/\sigma_0)$ against time or fluence and measuring the slope. $(\sigma_t/\sigma_0)$ is derived from from the radii of the stress relaxation beam as follows:

$$\frac{\sigma_t}{\sigma_0} = \frac{\frac{1}{R_t} - \frac{1}{R_h}}{\frac{1}{R_0} - \frac{1}{R_h}} \qquad (3)$$

where $\sigma_t$ and $\sigma_0$ are the stresses at a given fibre location at time t and time 0; $R_t$ and $R_0$ are the radii of the unconstrained beam at time t and time 0; and $R_h$ is the radius of the constrained beam in the holder.

## 1.2 Radiation Damage Analysis

Radiation damage is caused by the displacement of atoms producing vacant lattice sites (vacancies) and interstitial atoms (interstitials) referred to collectively as point defects. These defects can affect the material dimensions and the mechanical properties of an irradiated component. The point defects are mobile and flow to various sinks in the microstructure and also coalesce into vacancy or interstitial loops. The dislocation loops resist the motion of dislocations with a resulting increase in yield stress, a loss of ductility and toughness and a reduction in the contribution of the dislocation glide mechanism to creep. The mobile point defects tend to move to sinks to minimise the internal strain energy of the material and this leads to the relaxation of stresses in the irradiated component. This stress relaxation is often measured as a function of fast neutron fluence for in-reactor tests and these tests have been used as the basis to predict the in-reactor performance of reactor components such as the Inconel guide tube tensioning springs.

In the core of a nuclear reactor, most of the atomic displacement damage that gives rise to enhanced creep (stress relaxation) is caused primarily by direct collisions of fast neutrons with atoms in the components. Measurements of radiation exposure causing displacements are therefore often given as fast neutron fluxes for energies, E>1MeV. This measure is for comparison purposes only, applicable when spectra are similar, or as a guide to the approximate displacement damage one might expect for a given exposure. For example, the maximum energy of a primary knock-on for the Zr atom due to collision with a 1 MeV neutron is about 40 keV. A portion of this available energy is dissipated in ionisation and other processes that do not directly contribute to atomic displacements but the remainder is still sufficient to cause approximately 300 displacements [3]. Therefore the rate of stress relaxation for a component can often be assessed from in-reactor tests where the relaxation is measured as a function of fast neutron fluence (E>1MeV). However, such an evaluation is only strictly valid when the neutron spectrum for the component is identical to the test reactor spectrum. If the neutron spectra for the two cases are closely matched then one can be conveniently scaled to the other. When the spectra differ significantly then the displacement damage rates that are directly related to the irradiation creep rates have to be calculated.

In general, displacement of atoms due to irradiation can occur by a variety of processes. The three main processes that apply at the edge of the reactor core are: (i) direct displacement by collision with fast neutrons; (ii) recoil displacement from particle or photon emission (α, p and γ) after capturing a neutron; (iii) displacements caused by emitted particles or photons and by high-energy photons emanating from the core. For Ni-alloys in the reflector region of a CANDU reactor, where low energy neutrons dominate the neutron flux, the main mechanism for producing displacement damage is (ii).

The relative probability of causing an atomic displacement is given by a cross-section for a specific energy of the irradiating particle (e.g., neutron, photon, electron). Various sources for cross-section data are used: for neutrons, ENDF/B-VI nuclear library [4]; for electrons, Oak Ridge National Laboratory reports [5]; for gamma photons, NIST XCOM: Photon Cross-Section Database [6].

For most cases the radiation damage is calculated taking into account the main stable isotopes of the material. However for alloys containing large amounts of Nickel there is an additional component of displacement damage that arises by a secondary process involving the production of Ni-59 from Ni-58. This additional process also generates significant amounts of H and He [7,8]. The contribution from Ni-59 is not a significant enhancement to the total damage rate in the reactor core where most of the damage is caused by direct collisions with highly energetic neutrons. However, at the edge of the reactor, where the fast neutron flux is low and there is still a substantial flux of thermal neutrons, the contribution to the radiation damage involving Ni-59 can be significant. The relevant nuclear reactions are [9,10]:

$^{58}Ni(n,\gamma)^{59}Ni$ with $\sigma_0$ = 4.6 barns and resonance integral (>0.5 eV) = 2.2 barns;
$^{59}Ni(n,\gamma)^{60}Ni$ with $\sigma_0$ = 78 barns and resonance integral (>0.5 eV) = 120 barns;
$^{59}Ni(n,\alpha)^{56}Fe$ with $\sigma_0$ = 14 barns and resonance integral (>0.5 eV) = 20 barns;
$^{59}Ni(n,p)^{59}Co$ with $\sigma_0$ = 2 barns and resonance integral (>0.5 eV) = 3 barns;
$^{58}Ni(n,\alpha)^{55}Fe$ with $\sigma_0 \sim 0$ barns and resonance integral (>0.5 eV) = 0.12 barns;
$^{58}Ni(n,p)^{58}Co$ with $\sigma_0$ = 0 barns and resonance integral (>0.5 eV) = 0.81 barns,

$\sigma_0$ is the cross-section for neutrons with a velocity of 2200 $m.s^{-1}$ (0.025 eV). The half-life of Ni-59 is about 76000 years, and the atomic abundance of Ni-58 is 68.08% [10].

Although the ejected particles for each reaction themselves cause displacements, by far the biggest contribution to the displacement damage per event is the atom recoil. Details of the damage production for the (n,α), (n,p) and (n,γ) reactions are given in [7,8]. In these calculations the displacements due to the recoil and that caused by the ejected particle are factored in for the (n,α) and (n,p) reactions. Only the recoil effect is factored in to the damage production for the (n,γ) reaction. As the damage from γ-photons can be potentially important under certain conditions at the periphery of reactors [11,12] it is worthwhile to also consider the relative effect of the γ-photons.

In calculating the $\gamma$-induced atomic displacements the total $\gamma$-flux is a combination of $\gamma$-rays from the reactor core and those produced in the reactor or calandria walls via the (n,$\gamma$) reaction. Calculations by Bauman, [11], for $D_2O$ reactors showed that the additional displacement damage from the $\gamma$-rays produced in the reactor vessel walls could be up to a factor of three greater than the displacements due to $\gamma$-rays from the reactor core so the combined flux has to be used in calculations of the effect of $\gamma$-rays in the reactor vessel walls (or other peripheral components). In his study Bauman also showed that the $\gamma$-induced displacement damage could contribute another 15% of that due directly to prompt $\gamma$-recoil following thermal neutron capture. From the work at HFIR and elsewhere, it is particularly important to consider components made from ferritic stainless-steels (such as the end-fittings) because of the evidence showing that significant changes in mechanical properties occurred in these types of materials irradiated at relatively low temperatures (<373 K, for example) for doses of the order of $10^{-4}$ dpa [12].

The main process by which $\gamma$-rays produce displacement damage in nuclear reactor components is via the ($\gamma$,e) reaction. The high-energy electrons produced from this interaction subsequently produce the atomic displacements. Using the $\gamma$-ray spectrum and values for gamma interaction cross-sections producing electrons or positrons [6], and electron displacement cross-sections [5], estimates of $\gamma$-induced displacement damage rates were made, assuming:

1) The ($\gamma$,e) differential cross-sections for the for iron, nickel and chromium, (the principal elements present in the Inconel X-750) are within 10% of each other over the energy range of interest;

2) The electron energies are constant for a given $\gamma$-energy group and are related to the energy group;

3) The electron displacement cross-sections are for a threshold displacement energy ($E_d$) of 40 eV;

4) The stopping power (dE/dx) for electrons is $-3.75\times10^3$ MeV.m$^{-1}$ for 1.5 MeV electrons in Zr [13] and is assumed to be representative for the range of electron energies of interest here, i.e. up to 12 MeV. The stopping power for Ni, Fe and Cr is calculated from the Zr value assuming that it is proportional to electron density, e.g. stopping power for Fe is 1.29 larger than that of Zr (assuming a mass density for Fe of 7.9 g.cm$^{-3}$ compared with 6.5 g.cm$^{-3}$ for Zr);

5) The $\gamma$-ray spectrum and flux is assumed constant over the region of interest where the $\gamma$-ray flux and spectrum is defined.

The number of electrons of energy, E, produced per atom by the ($\gamma$,e) interaction for a given $\gamma$-ray flux ($\phi_\gamma$ particles.cm$^{-2}$), $n_e(E)$, is given by:

$$n_e(E) = \Omega.\phi_\gamma.\sigma_{(\gamma,e)}(E) \quad (4)$$

where $\sigma_{(\gamma,e)}(E)$ is the differential cross-section for electron production in cm$^{-1}$, and $\Omega$ is the atomic volume in cm$^3$ (typically about $10^{-23}$ cm$^3$). There are three types of ($\gamma$,e) events to consider [14]: pair-production (pp); the photoelectric process (pe); and Compton scattering (cs).

The number of displacements per atom (dpa) produced by the ($\gamma$,e) interaction is then the product of the number of displacements per electron of energy E, $n_d(E)$, and the number of electrons per atom, $n_e(E)$, defined above. The probability (p) that a given atom is displaced by an electron with energy E is given by:-

$$p(E) = (1/\Omega).\sigma_d(E).dx \quad (5)$$

where $\sigma_d(E)$ is the atomic displacement cross-section for electrons with energy E.

The electron with initial energy, $E_i$, loses energy throughout its trajectory and therefore the total number of displacements per electron is given by:

$$n_d(E_i) = \int_0^{E_i} \frac{(1/\Omega)\sigma_d(E)\,dE}{-dE/dx} \qquad (6)$$

where the subscript i refers to each of the (γ,e) events, pp, pe and cs. The total number of displacements per atom (dpa) produced as a result of the (γ,e) reaction within a Ni, Fe and Cr - based component is therefore:

$$\text{dpa} = \Sigma_i\, n_d(E_i).\, n_e(E_i) \qquad (7)$$

## 2. Experimental Data

The X-750 material subject to in-reactor stress relaxation measurements was hot-rolled plate given a final aging treatment of 24h at 977 K [1]. Metallography and hardness tests showed a microstructure with equiaxed grains with frequent occurrences of annealing twins along with some carbide particles, Figure 2.

The experimental procedures used for in-reactor bent-beam stress-relaxation experiments have been described in detail elsewhere [2]. The test involves determining the amount of stress relaxed during irradiation in a given time from periodic out-reactor measurements. The initial elastic stress is determined from the curvature of a constrained beam that is bent to a given curvature prior to irradiation. The relaxed stress is determined from the unconstrained curvature of the small beam after removal at each stage of the irradiation, Figure 3.

Samples were irradiated in flowing water in NRU in fast (E> 1 MeV) neutron fluxes of about 1.5 to 1.8 x $10^{17}$ n/m$^2$/s at two nominal temperatures, 330 K and 570 K. The stress relaxation results at 330 K and 570 K for samples taken from the rolling direction of the Inconel X-750 plate are plotted in Figure 4. The ratio of initial to relaxed stress is plotted against fast neutron fluence, E>1MeV. Previous data reported by Causey et al. [1] indicated that the relaxation rate of this material was typically higher at 330 K than at 570 K by a factor of about two. The data reported here are for the same samples but include more points at higher fluences. The present data confirm the previous trend and also correct for an erroneous data point in the previously reported results [1]. The inverse temperature dependence is rather surprising but has been observed both in Ni-alloys and in austenitic stainless steels [1, 15] and supports the assumption that irradiation effects dominate the creep.

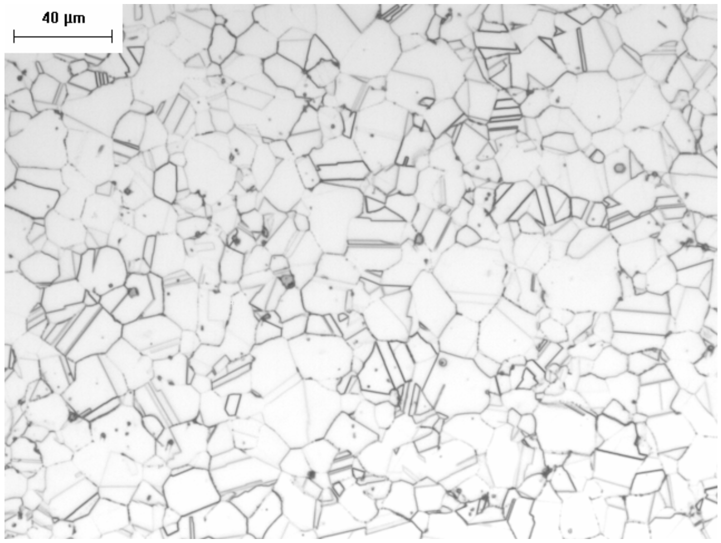


Figure 2. Grain structure of Inconel X-750.

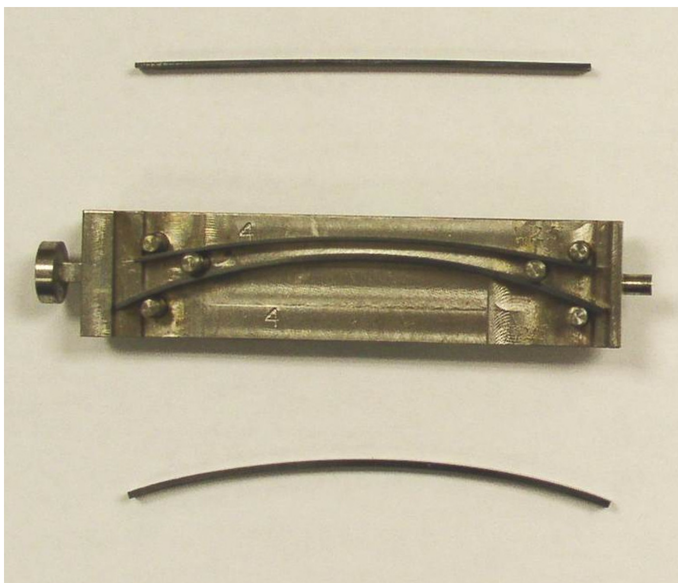

Figure 3. Specimens and specimen holder used to assess stress-relaxation. An untested specimen is shown at top. The same type of specimen but mounted in a four-point bending jig is shown centre. The permanent deformation after irradiation is shown at bottom.

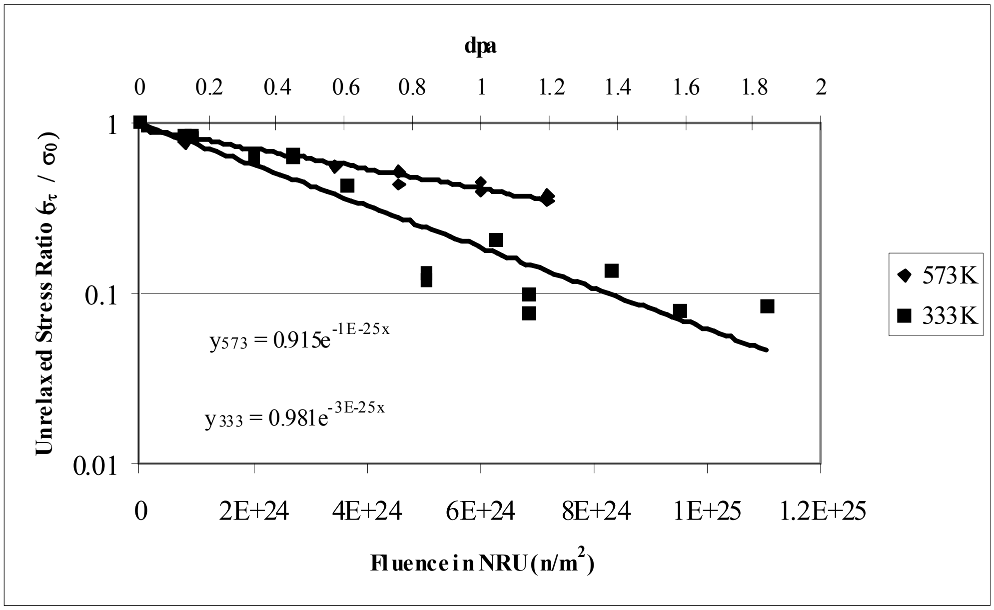


Figure 4. Stress relaxation data from samples of hot finished and aged Inconel X-750.

## 3. Results and Discussion

Atomic displacement rate calculations were performed for Inconel X-750 (an alloy of Ni, Cr and Fe with nominal weight fractions 0.74Ni-0.17Cr-0.09Fe) with the neutron spectra in NRU and the spectra coinciding with the tensioning spring in the reflector region of the CANDU reactor. Two aspects of the radiation damage production were considered: (1) the relative contributions to atomic displacement from the fast, thermal and gamma fluxes as a function of axial location (along the spring component) at the reactor periphery based on the most abundant isotope for each element in the alloy; (2) the relative dpa rate at the mid-point of the Inconel X-750 spring component compared with that in material test positions in the NRU test reactor from which the relaxation rate in the spring will be assessed taking into account the effect of transmutation of Ni-58 to Ni-59.

### 3.1 Calculation of dpa Rate at CANDU Reactor Periphery Using Abundant Isotopes.

The neutron fluxes and corresponding dpa rates were determined for a radial mesh in the mid-plane of the core with mid-point mesh positions at about 328 cm and 349 cm from the centre of the reactor core, approximately corresponding to the top and bottom of the Inconel X-750 spring component. The neutron energy groups were matched to the group structure of the displacement cross sections used for the analysis and the dpa rates were calculated for Inconel with the above composition. The neutron and gamma fluxes are shown in Figure 5. Figure 6 compares the total displacement rate due to: (i) direct collisions (fast neutrons, E>580 eV); (ii) prompt $\gamma$-recoil after neutron capture (thermal neutrons); and (iii) $\gamma$-photons. For Ni, the minimum neutron energy needed to cause direct displacement damage is 580 eV when the atomic displacement threshold energy is 40 eV.

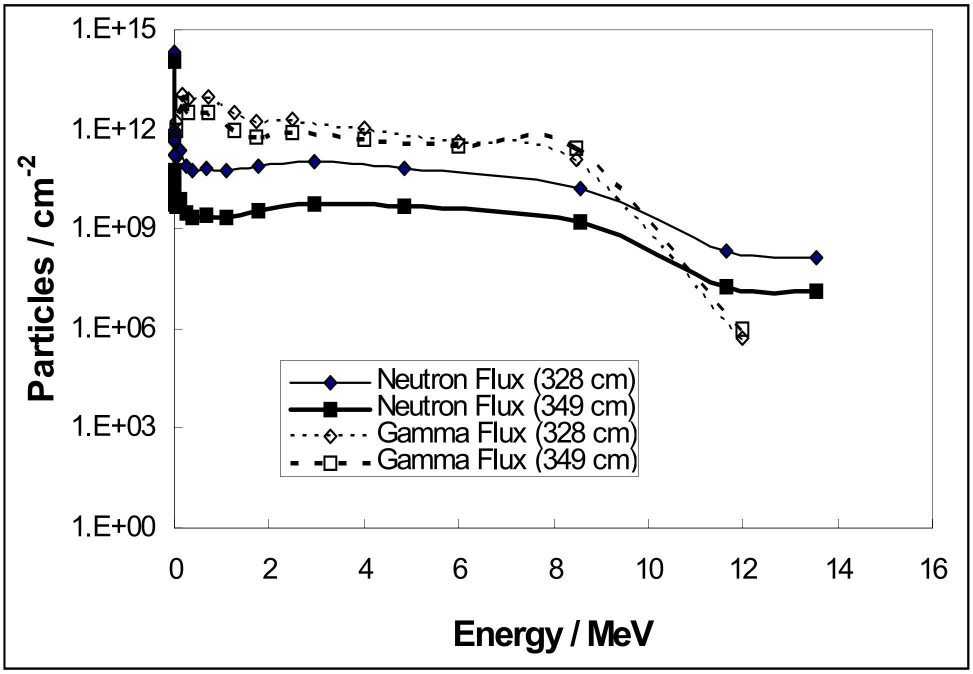


Figure 5. Gamma and neutron spectra at the top and bottom of an Inconel X-750 tensioning spring at the periphery of a CANDU reactor.

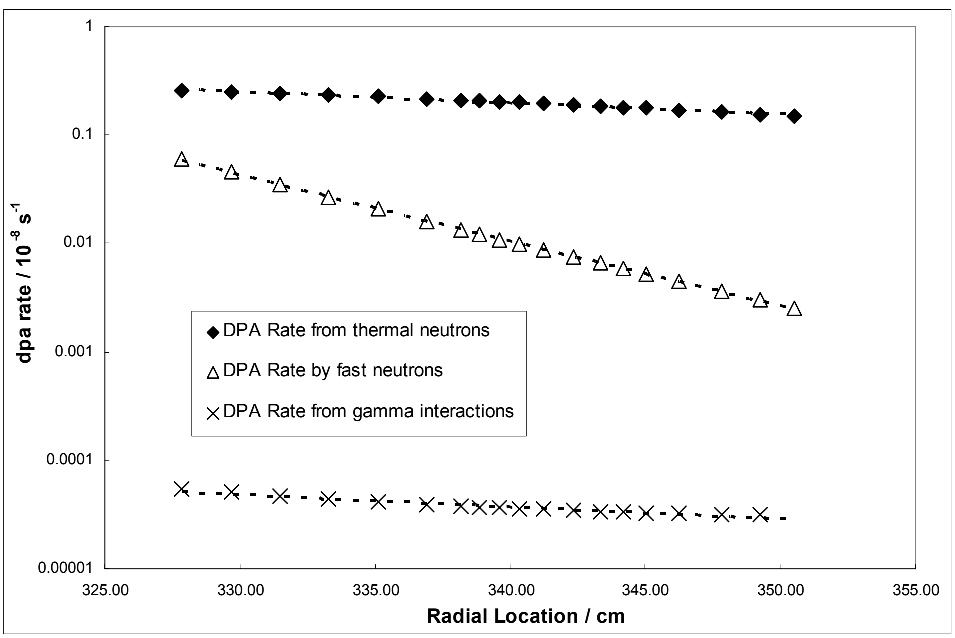


Figure 6. Displacement rates for Inconel as a function of radial location in the reactor core mid-plane based on the natural stable isotope mix.

The results show that the atomic displacements due to thermal neutron capture with subsequent photon emission can be 1 to 2 orders of magnitude greater than the displacements caused by direct fast neutron collisions. The results also show that the photon-damage effect is negligible compared with either the fast or thermal neutron effects. Figure 7 shows the neutron spectra at the centre of the Inconel spring compared with a central location in the core (mid-way between the pressure tubes and calandria tubes). It is clear that there is a much lower fast neutron flux at the spring compared with the core although the thermal flux is much the same. The transition from the periphery (where the damage production is dominated by the thermal flux) towards the reactor core (where the fast neutron flux dominates damage production) is illustrated in Figure 8.

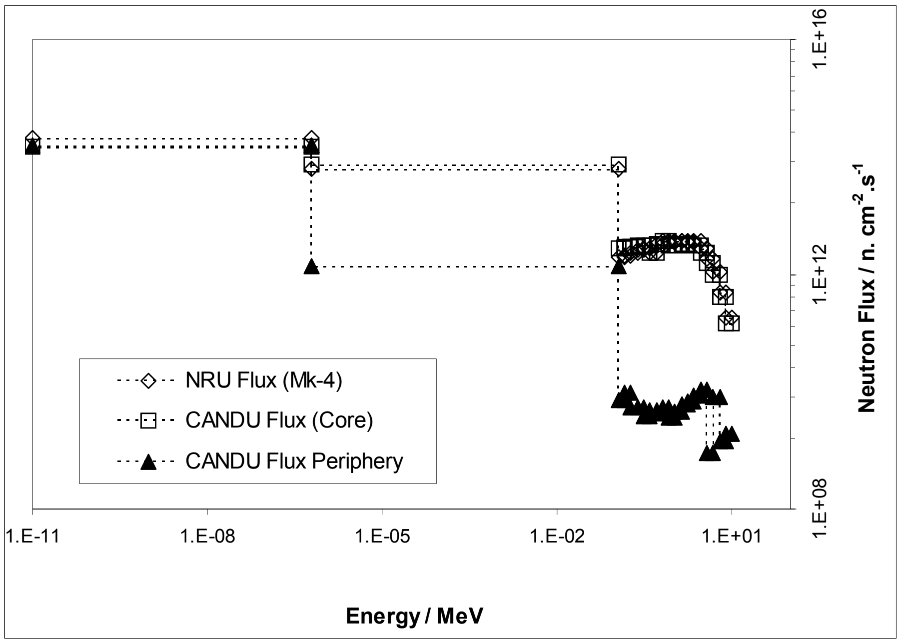


Figure 7. Neutron spectra at the centre of an Inconel X-750 tensioning spring at the periphery of a CANDU reactor compared with the core of a CANDU reactor and a Mk-4 irradiation test site in NRU.

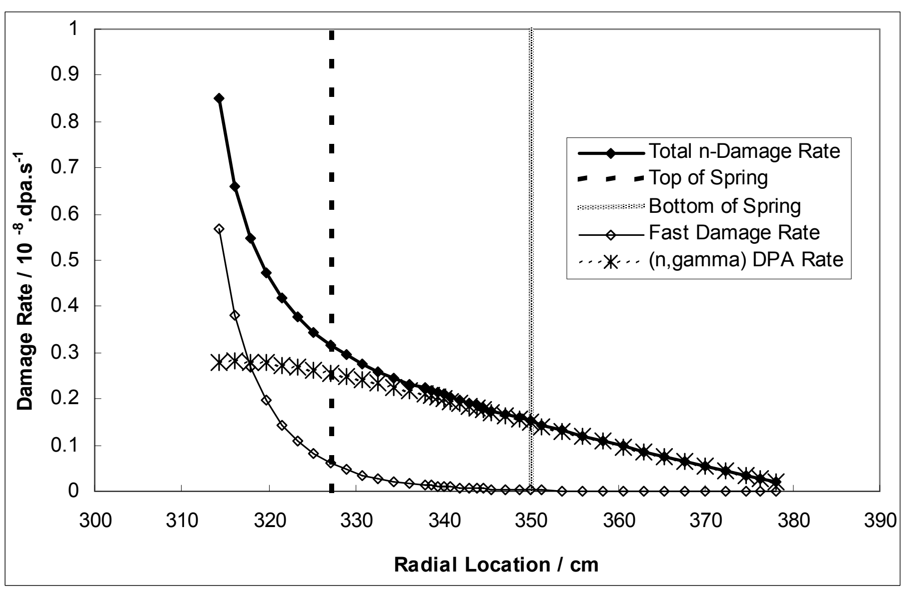


Figure 8. Displacement rates for Inconel as a function of radial location in the reactor core mid-plane.

## 3.2 Calculation of dpa Rate at CANDU Reactor Periphery compared with NRU Mk-4 taking into account the effect of transmutation of Ni-58 to Ni-59

Figure 7 shows the neutron spectrum for the NRU Mk-4 test insert in the NRU reactor. Because the spectra are similar, to a large extent experiments conducted in the NRU Mk-4 insert can be used to predict the behaviour of components in CANDU reactor cores simply by extrapolating the results based on the neutron fluence. Although the NRU Mk-4 test insert reproduces the neutron spectrum that is similar to the core of a CANDU reactor it is not comparable with the spectrum at the edge of the core. For this reason any assessment of material performance based on the Mk-4 tests have to be normalised to dpa in order to predict the behaviour at the periphery of the core.

Rigorous dpa calculations were performed corresponding with the Mk-4 insert used for the stress-relaxation experiments described in Section 2 and compared with a location 340 cm from the centre of the reactor core. The calculations were performed taking into account the transmutation of Ni-58 to Ni-59 with subsequent additional (n,p) and (n,α) processes producing a significant additional component to the total damage. The dpa production for Inconel X-750 irradiated in NRU with and without taking into account the Ni-59 production is shown in Figure 9. A similar plot for the centre of the Inconel spring at the periphery of the CANDU reactor is shown in Figure 10. The results show that including the Ni-59 in dpa calculations does not affect the analysis significantly for irradiations in NRU Mk-4 for low doses (<5 dpa). However, for the irradiation on the periphery of the core there is a significant contribution from Ni-59.

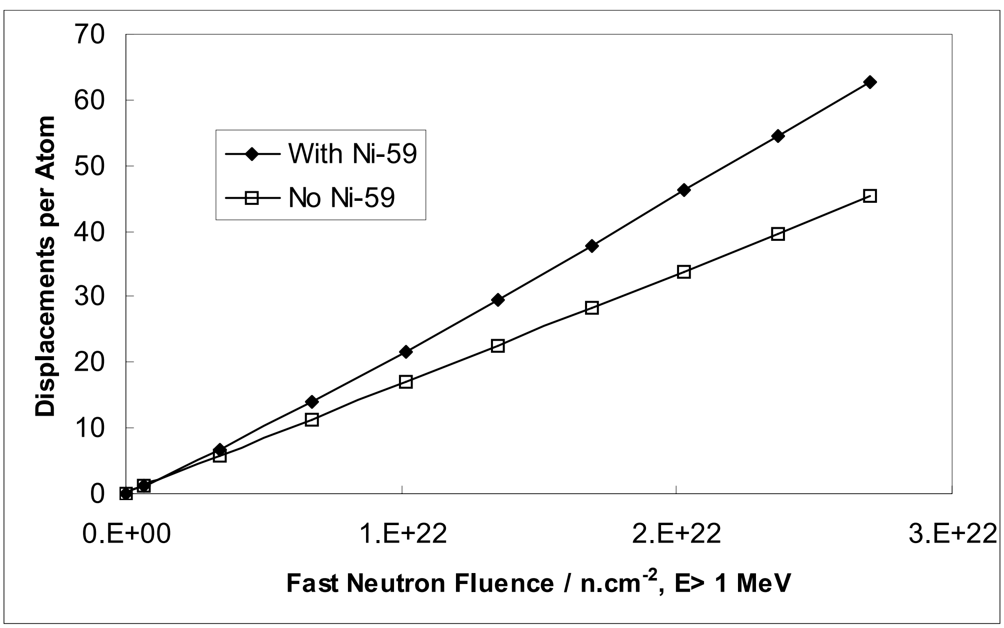


Figure 9. Displacement rates for Inconel X-750 relative to fast neutron flux for the Mk-4 cavity in NRU. The two plots illustrate the effect of not including Ni-59 in the calculation – not significant at low doses.

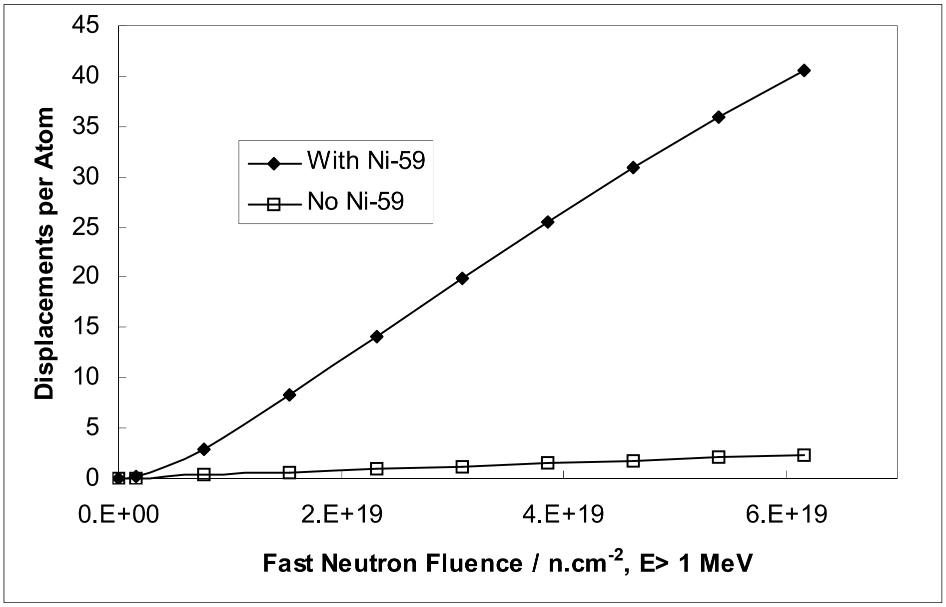


Figure 10. Displacement rates for Inconel X-750 relative to fast neutron flux at the periphery of a CANDU reactor core. The two plots illustrate the effect of not including Ni-59 in the calculation –significant even at low doses.

The data shown in Figure 4 show that relaxation of Inconel X-750 at 330K is >90% after about 2 dpa (this includes the effect of Ni-59). The dose or fast neutron fluence to achieve 2 dpa is approximately 1.1 x $10^{21}$ n.cm$^{-2}$, E > 1 MeV for an irradiation in NRU. If fast neutron damage was used to scale the relaxation phenomenon, a fast neutron fluence of 1.1 x $10^{21}$ n.cm$^{-2}$ (E > 1 MeV) would be achieved at the centre of the tensioning spring after about 650 effective full-power years of service. On this basis the expected relaxation of the tensioning spring relative to the irradiation in NRU is shown in Figure 11. However, when considering the contributions to displacement damage from the various interactions with thermal neutrons, a dose of 2 dpa is achieved at the centre of the Inconel spring after only a slightly longer irradiation time compared to the NRU irradiation, Figure 12, i.e. after about 3 effective full-power years of service in the CANDU reactor (this value would have been about 40 effective full-power years when considering damage from Ni-58 only, Section 3.1). The data shown in figures 11 and 12 clearly illustrate that fast neutron fluence is not an appropriate scaling parameter when predicting material behaviour based on tests in materials test reactors. A dpa calculation is required in order to be able to compare irradiation doses in different reactor environments. The results also show that in the case of Ni–containing alloys it is important to perform the dpa conversion taking into account the Ni-59 production.

## 4. Conclusions

Apart from showing that the total displacement dose in the tensioning spring is sufficient to give considerable relaxation, the main finding is that neutron capture is the primary contribution to radiation damage in Inconel X-750 tension springs located at the edge of the CANDU core. Not only is there a significant contribution to displacements caused by atom recoil associated with photon emission, but more significantly in the case of Ni, the process of transmutation giving Ni-59 is a major contributor to the damage process. Since the neutron spectrum at the periphery of the reactor core is quite different from that within the core, or when compared with materials test reactors, it is important to calculate the atomic displacement rate from accurate spectra data and multigroup damage cross sections taking into account transmutation processes.

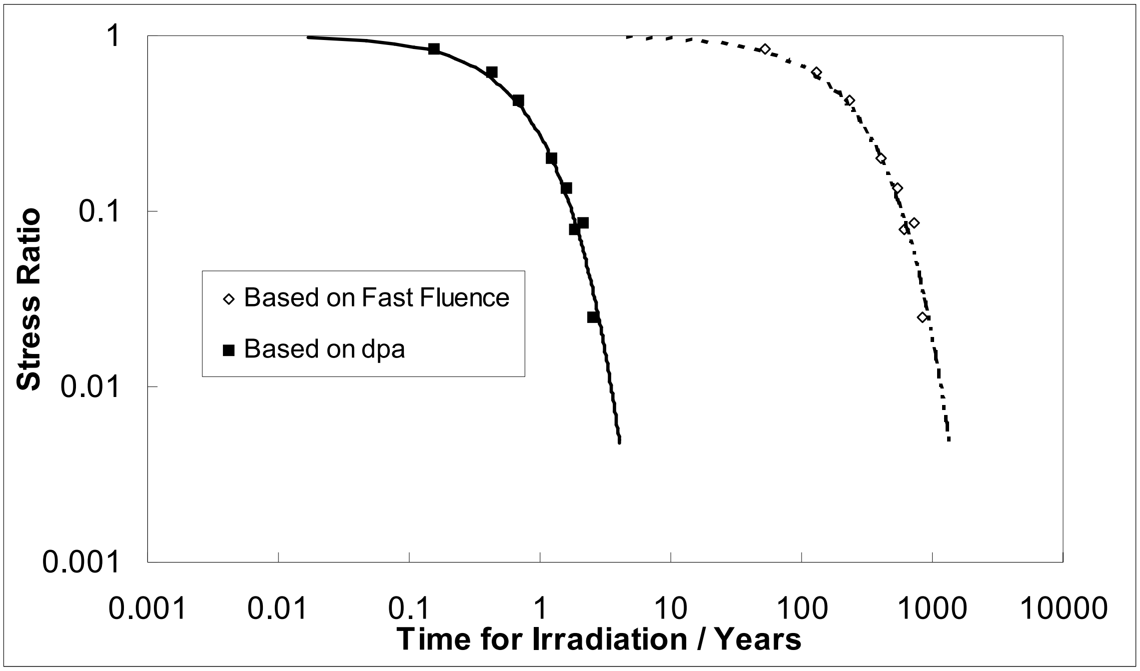


Figure 11. Time for stress relaxation for Inconel X-750 when using fast fluence (E>1MeV) to normalise.

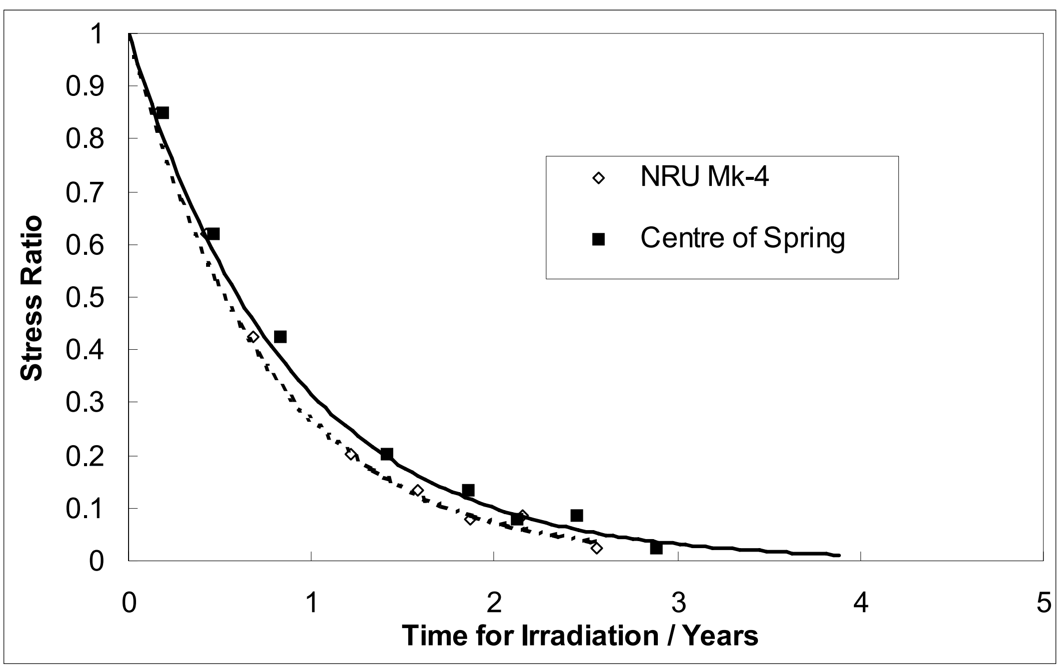


Figure 12. Time for stress relaxation for Inconel X-750 when using dpa to normalise.

**Acknowledgements**

The authors would like to thank Charles Boss, Stephen Donohue, Bruce Wilken and Marc Leger for useful discussions in connection with this work.

**References**

[1] A.R. Causey, G.J.C. Carpenter and S.R. MacEwen, “In-Reactor Stress Relaxation of Selected Metals and Alloys at Low Temperatures”, Journal of Nuclear Materials 90 (1980) pp 216-223.

[2] D.E. Fraser, P.A. Ross-Ross and A.R. Causey, “The Relation Between StressRelaxation and Creep For Some Zirconium Alloys During Neutron Irradiation”, Journal of Nuclear Materials 46(1973) pp 281-292.

[3] M.J. Norgett, M.T. Robinson and I.M. Torrens, “A Proposed Method of Calculating Displacement Dose Rates”, Nucl. Eng. And design, 33 (1975) p. 50-54.

[4] ENDF/B-VI nuclear library, Available from: URL: http://t2.lanl.gov.

[5] O.S. Oen, "Cross Sections for Atomic Displacements in Solids by Fast Electrons", USAEC unclassified report. ORNL-3813 (1965).

[6] NIST XCOM: Photon Cross-Section Database, Available from: URL: http://physics.nist.gov.

[7] L.R. Greenwood, “A new calculation of Thermal Neutron Damage and Helium Production in Nickel”, Journal of Nuclear Materials 115 (1983), pp. 137-142.

[8] L.R. Greenwood and F.A. Garner, “Hydrogen Generation arising from the $^{59}$Ni(n,p) Reaction and its impact on Fission-Fusion Correlations”, Journal of Nuclear Materials 233-237 Part 2 (1996), pp. 1530-1534.

[9] W. B. Wilson, et al., CINDER’90 code for Transmutation Calculations, International Conference on Nuclear Data for Science and Technology, Trieste, May 19-24, 1997, Conference Proceedings, vol.59, Part II, p. 1454-1457, 1997.

[10] 16th edition Nuclides and Isotopes, Chart of Nuclides, KAPL, (2002), Available from: URL: http://www.nndc.bnl.gov/chart.

[11] N.P Baumann, "Gamma-ray Induced Displacements in $D_2O$ Reactors", Proc. of 7$^{th}$ ASTM-EURATOM Symp. on Reactor Dosimetry, Strasbourg, Kluwer Academic Publ., Dordecht, p 689, 1990. Also under report: WSRC-RP-89-619; CONF-900814-18.

[12] I. Remec, J.A. Wang, and F.B.K. Kam, "HFIR Steels Embrittlement: The Possible Effect of Gamma Field Contribution", Effects of Radiation on Materials: 17$^{th}$ International Symposium, ASTM STP 1270, p 591-605, 1996.

[13] G.M. Hood, H.E. Hansen and R.J. Schultz, "A Positron Annihilation Spectroscopy Determination of Defect Depth Distribution Profiles in Electron Irradiated Zr and Ti", Radiation Effects And Defects in Solids, Vol. 91 (1985) p 111-124.

[14] M.W. Thompson, "Defects and Radiation Damage in Metals", Cambridge University Press (1969).

[15] M. L. Grossbeck and L.K. Mansur, “Low-temperature Irradiation Creep of Fusion Reactor Structural Materials”, J. Nucl. Mater., 179-181Part 1 (1991) p. 130-134.